

PepMLM: Target Sequence-Conditioned Generation of Peptide Binders via Masked Language Modeling

Tianlai Chen,^{1,*} Sarah Pertsemlidis,^{1,*} Rio Watson,¹ Venkata Srikar Kavirayuni,¹ Ashley Hsu,¹ Pranay Vure,¹ Rishab Pulugurta,¹ Sophia Vincoff,¹ Lauren Hong,¹ Tian Wang,¹ Vivian Yudistyra,¹ Elena Haarer,¹ Lin Zhao,¹ Pranam Chatterjee^{1,2,3,†}

1. Department of Biomedical Engineering, Duke University
2. Department of Computer Science, Duke University
3. Department of Biostatistics and Bioinformatics, Duke University

*These authors contributed equally

†Corresponding author: pranam.chatterjee@duke.edu

Abstract

Target proteins that lack accessible binding pockets and conformational stability have posed increasing challenges for drug development. Induced proximity strategies, such as PROTACs and molecular glues, have thus gained attention as pharmacological alternatives, but still require small molecule docking at binding pockets for targeted protein degradation (TPD). The computational design of protein-based binders presents unique opportunities to access “undruggable” targets, but have often relied on stable 3D structures or predictions for effective binder generation. Recently, we have leveraged the expressive latent spaces of protein language models (pLMs) for the prioritization of peptide binders from sequence alone, which we have then fused to E3 ubiquitin ligase domains, creating a CRISPR-analogous TPD system for target proteins. However, our methods rely on training discriminator models for ranking heuristically or unconditionally-derived “guide” peptides for their target binding capability. In this work, we introduce **PepMLM**, a purely target sequence-conditioned *de novo* generator of linear peptide binders. By employing a novel masking strategy that uniquely positions cognate peptide sequences at the terminus of target protein sequences, PepMLM tasks the state-of-the-art ESM-2 pLM to fully reconstruct the binder region, achieving low perplexities matching or improving upon previously-validated peptide-protein sequence pairs. After successful *in silico* benchmarking with AlphaFold-Multimer, we experimentally verify PepMLM’s efficacy via fusion of model-derived peptides to E3 ubiquitin ligase domains, demonstrating endogenous degradation of target substrates in cellular models. In total, PepMLM enables the generative design of candidate binders to any target protein, without the requirement of target structure, empowering downstream programmable proteome editing applications.

Introduction

The development of therapeutics largely relies on the ability to design small molecule- or protein-based binders to pathogenic target proteins of interest.¹ These binders can either be used as inhibitors or as functional recruiters of effector enzymes.² For example, proteolysis targeting chimeras (PROTACs) or molecular glues are heterobifunctional small molecules that bind and recruit endogenous E3 ubiquitin ligases for targeted protein degradation (TPD).^{3,4} Still, these small molecule-based methods rely on the existence of accessible cryptic or canonical binding sites, which are not present on classically “undruggable” intracellular proteins.^{5,6} With the advent of deep learning-based structure prediction tools such as AlphaFold2,⁷ combined with generative modeling,¹ algorithms such as RFDiffusion and MASIF-Seed enable researchers to conduct *de novo* protein binder design from target structure alone.^{8,9} Nonetheless, much of the undruggable proteome, including dysregulated proteins such as transcription factors and fusion oncoproteins, are conformationally disordered, thus biasing design to a small subset of disease-related proteins.^{1,6}

Over the past few years, deep learning has revolutionized natural language processing (NLP), particularly through the implementation of the attention mechanism.¹⁰ This foundational advancement has transcended the boundaries of natural language analysis, finding pertinent applications in the modeling of other languages, such as proteins, which are fundamentally sequences of amino acids.¹¹ In recent times, several protein language models (pLMs), trained on distinct transformer architectures, such as ProtT5, ProGen2, ProtGPT2, and the ESM series, have accurately captured critical physicochemical properties of proteins.^{12–15} Notably, ESM-2 currently stands as the state-of-the-art model in the realm of protein sequence encoding, essentially functioning as a BERT-style model that discerns co-evolutionary patterns among protein sequences via a masked language modeling (MLM) training task.^{16,17} These models have been extended to powerful applications, including antibody design, the creation of novel proteins, and structure prediction, offering a streamlined approach to embedding useful protein information.^{13,14,16,17} Recently, our lab has leveraged the expressivity of pLMs to both generate and prioritize effective peptidic binder motifs to targets of interest, enabling design of peptide-guided degraders, termed ubiquibodies (uAbs).^{18–20} As such, uAbs represent a programmable, CRISPR-like approach for TPD. Our early models, Cut&CLIP and SaLT&PepPr, rely on the existence of interacting partner sequences as scaffolds for peptide design.^{19,20} Most recently, our PepPrCLIP model generates *de novo* peptides by first sampling the ESM-2 latent space for naturalistic peptide candidates, and then screening these candidates through a contrastive model to determine target sequence specificity.²¹ However, a purely *de novo*, target sequence-conditioned binder design algorithm has yet to be developed.

To achieve this goal, we introduce **PepMLM**, a novel Peptide binder design algorithm via Masked Language Modeling, built upon the foundations of ESM-2.¹⁶ PepMLM innovates by employing a contiguous masking strategy that uniquely positions the entire peptide binder sequence at the terminus of target protein sequences, compelling ESM-2 to reconstruct the entire binding region (Figure 1A). PepMLM-derived linear peptides achieve low perplexities, matching or improving upon validated peptide-protein sequence pairs in the test dataset, outperform the state-of-the-art RFDiffusion model for peptide generation on structured targets *in silico*,⁸ and experimentally exhibit degradation capability of endogenous, disordered target substrates when incorporated into the uAb architecture. Overall, by focusing on the complete reconstruction of peptide regions, PepMLM represents the first example of target-conditioned *de novo* binder design from sequence alone, thus facilitating a deeper understanding of binding dynamics and paving the way for the development of more effective, targeted binders to unstructured proteins of interest.

Results

We trained PepMLM using existing peptide-protein binding data sourced from the recent PepNN training set and the gold-standard Propedia dataset.^{22,23} We subjected our curated dataset to a filtration process based on the lengths of the binder and target protein sequences, which were confined to 50 and 500 respectively. To remove redundancies, we applied a homology filter thresholded at 80%, resulting in a final training set of 10,000 samples and leaving 203 samples for testing.²⁴ Each entry in the dataset comprised a concatenated protein and binder sequence. During the training phase, we masked the entire peptide sequence, tasking the model to reconstruct them via the ESM-2-650M model. The discrepancy between the ground truth binder and the reconstructed binder induces a cross entropy loss, thereby forcing parameter updates via gradient descent.

Post fine-tuning, we generate peptide binders of specific lengths by providing the model with a target protein sequence and a user-defined number of mask tokens, as illustrated in Figure 1A. Final settings and hyperparameters used to train our model are presented in Supplementary Table 1.

We considered two distinct decoding strategies during the generation phase. The default strategy, akin to ESM-2 or BERT-style models,¹⁶ employs greedy decoding, wherein the token with the highest probability is selected at each site. Despite its efficacy, greedy decoding is limited to the generation of a single peptide binder. To augment the diversity of the peptides, we introduced top- k sampling, allowing PepMLM to randomly select from the top k probable tokens at each site. In this decoding strategy, we evaluated perplexity alongside various k values, ranging from 2 to 10, on the test set of target proteins. For each target protein, we generated 10 binders of the same length as the ground truth binder. We observed that as k increased, perplexity also rose, indicating a decrease in model confidence (Supplementary Figure 1). While higher k values yielded more diverse binder sequences, they also corresponded with an increase in the number of outliers. To find a balance between sequence diversity and maintaining model confidence (as indicated by the lower perplexity), we settled on $k = 3$ as our final selection.

To substantiate the efficacy of the generated peptides, we conducted a comprehensive series of computational benchmarks with test set peptide-target pairs. The total 203 test set target proteins were utilized to generate one peptide binder each, employing pre-trained ESM-2 embeddings and PepMLM. Subsequently, the pseudo-perplexity of the binder region was computed for four groups of target protein:binder pairs. For a majority of the test set, known binders exhibited a reasonable perplexity range, with only a few outliers (those with a perplexity > 40), validating the PepMLM's effective ability to model them accurately (Figure 1B and Supplementary Table 2). A comparative analysis revealed that the binders generated by PepMLM exhibited lower perplexity values, suggesting a higher likelihood of them making stable binding interactions with the target (Figure 1B). Moreover, our distribution analysis revealed that PepMLM closely mirrors the distribution peak of real binders, a deviation from the distribution shifts observed with the original ESM-2 model alone and with randomly generated binders (Figure 1C). Among the generated candidates, five exemplary generated binder and protein complexes, which exhibited promising ipTM scores, are illustrated in Figure 1D. They are colored according to pLDDT and were co-folded utilizing AlphaFold-Multimer through ColabFold.²⁵ This observation highlights the model's proficiency in capturing the inherent conditional distribution associated with protein and peptide binding.

Next, to benchmark PepMLM's generation quality, we co-folded the test and generated binders with their respective target proteins utilizing AlphaFold-Multimer, which has been proven effective at predicting peptide-protein complexes.^{26,27} The pLDDT and ipTM scores, verified metrics within AlphaFold2,⁷ function as critical indicators of the structural integrity and the potential interface binding affinity of peptide-protein complex, respectively, providing a quantitative assessment of our generation. The extracted ipTM and pLDDT values from our benchmarking indicated a statistically significant negative correlation ($p < 0.01$) with PepMLM perplexity, affirming the model's reliability at prioritizing binders with stable binding capacity to the target (Supplementary Figure 2). Subsequent analysis involved sorting the test set based on their ipTM values and contrasting these with the ipTM values of the associated PepMLM-generated binders. Our analysis yielded a hit rate exceeding 38% (Figure 2A). When applying the same evaluation process to RFDiffusion for binder design on the test set, the hit rate was below 30% (Figure 2B), suggesting PepMLM's comparative advantage in designing peptide binders, potentially reducing the need for extensive downstream experimental screening.

To corroborate our *in silico* results on more unique targets, we first sought to test PepMLM-generated binders in our uAb architecture to degrade pathogenic proteins in a cellular model of Ewing sarcoma, a pediatric bone malignancy with no approved targeted therapies.²⁸ As our targets, we chose two cancer-related proteins, 4E-BP2 and β -catenin, as well as the more structured histone H3 protein, a core epigenetic nuclear protein that comprises chromatin.²⁹⁻³¹ To design peptides, we first employed greedy decoding to determine the optimal binder length that yielded the lowest perplexity, followed by the generation of binders for each target sequence using top k sampling, where k was fixed at 3 as previously described (Supplementary Table 3). After cloning these peptides into our uAb backbone and transfecting into A673 Ewing sarcoma cells, we conducted Western blotting on whole-cell protein extracts with target-selective primary antibodies (Figure 2C). Our results demonstrate that select PepMLM-generated "guide" peptides induce binding and subsequent degradation of

endogenous targets when fused to E3 ubiquitin ligase domains, demonstrating reduced protein levels relative to that of the non-targeting control uAb (Figure 2D and Supplementary Figure 3). Next, we sought to compare PepMLM-derived degraders with that of RFDiffusion on TRIM8, a known regulator of the fusion oncoprotein, EWS-FLI1, that drives Ewing sarcoma.³² For both models, we generated 15 amino acid binders provided the target sequence (to PepMLM) or target structure (to RFDiffusion) of TRIM8 (Supplementary Table 4). After integrating these peptides into uAb-expressing plasmids, we evaluated TRIM8 protein degradation via Western blotting and observed comparable performance between the two models (Figure 2E). In total, our results motivate further design and testing of effective PepMLM-derived degraders to diverse pathogenic targets, whether they are conformationally stable or not.

To this point, we had utilized the lightweight ESM-2-650M model, enabling flexible fine-tuning and inference. To assess the performance of larger models, we additionally fine-tuned ESM-2-3B¹⁶ for peptide generation (PepMLM-3B) and evaluated it using the same methodology as employed for the ESM-2-650M version of PepMLM (PepMLM-650M). However, as illustrated in Supplementary Figure 4, we did not observe a substantial improvement in either perplexity or hit rate for PepMLM-3B (36.02%). Considering the associated resource and inference costs, we provide our PepMLM-650M model as an accessible resource for effective linear peptide generation.

Discussion

By simply redesigning a guide RNA, the CRISPR-Cas system enables targeting and modification almost any DNA sequence, a programmable process that has revolutionized biology.³³ Specifically, with the recent engineering of protospacer adjacent motif (PAM)-relaxed Cas variants, there is minimal restriction as to which user-defined DNA sequences can be bound and edited.^{34,35} Unfortunately, an analogous, programmable system for “editing” proteins has yet to be developed, as the design of target-specific binders requires either accessible binding pockets for small molecules, which do not exist on “undruggable” targets such as those at flat protein-protein interaction interfaces, or conformationally-stable 3D structures, precluding the binding of disordered targets such as dysregulated transcription factors and fusion oncoproteins.¹ To mitigate these shortcomings, here, we introduce PepMLM, the first *de novo* binder design algorithm directly conditioned on the target sequence of a protein. By using generated peptides as guides for E3 ubiquitin ligase domains, and eventually other post-translational modification domains, this work serves as a step forward towards developing a fully modular proteome editing system.

We envision that further improvements can be made to PepMLM, enabling its adoption as a universal tool for peptide binder design. For example, PepMLM can be retrained with modification-aware and variant-aware pLM embeddings to enable specificity to post-translational isoforms over wild-type protein states. We also plan to integrate PepMLM generation with high-throughput lentiviral screening to both evaluate its hit rate experimentally and input experimental data back into the algorithm, creating an active learning-based optimization loop. As a note, we have not validated PepMLM’s ability to generate high affinity, standalone peptide binders, those that can be further stabilized via cyclization or stapling, though this may prove possible via the current algorithm.^{36,37} Nonetheless, we envision that through additional development, our accessible peptide generator, coupled with variants of our uAb architecture, will enable a CRISPR-analogous system to bind and modulate any target protein, whether structured or not.

Methods

Data Curation

In the data curation phase, protein and peptide complexes were amalgamated from the PepNN and Propedia databases.^{22,23} Initially, redundancy between the two datasets was eliminated, followed by the utilization of MMseqs2 to cluster the remaining protein sequences, setting a threshold of 0.8.²⁴ When protein sequences were identified within the same cluster and exhibited identical binder sequences, a single sequence was retained. This was followed by a manual filtering process, wherein protein sequences were sorted and those exhibiting high similarity (threshold of 80%) were removed to further mitigate homology issues. Consequently, a dataset comprising 10,203 entries was amassed, from which 10,000 were randomly allocated for training and

203 for testing. The maximum lengths for the binder and protein sequences were established at 50 and 500, respectively.

Conditional Peptide Modeling

Peptide binders are modeled in a distinctive manner, wherein the peptides are modeled conditionally based on the full protein sequence. Let $p = (p_1, p_2, p_3, \dots, p_n)$ represent the target protein sequence of length n and $b = (b_1, b_2, b_3, \dots, b_m)$ denote the binder of length m . The protein and peptide sequences are concatenated, incorporating special tokens of start, end, and padding. Mask language modeling transforms this into a conditional modeling problem, where the objective is to reconstruct b given p , as the entire b region is masked during both training and generation phases. The entire model is updated with Cross Entropy loss, which can be represented as:

$$\mathcal{L} = - \sum_{i=1}^m b_i \log(\hat{b}_i)$$

Through this methodology, the discrepancy between the generated binders and the ground truth is minimized, facilitating the learning of the conditional probability, $\prod_{i=1}^m P(b_i|p)$.

PepMLM Training

The pre-trained protein language model, ESM-2, was utilized to facilitate full parameter fine-tuning. ESM-2, a transformer-based model, is adept at discerning coevolutionary patterns across protein sequences. The concatenated protein and peptide sequences were tokenized at the amino acid level and input into the model. Deviating from the original training strategy of ESM, the entire binder sequence was exclusively masked, compelling the model to learn the relationship between the peptide binder and the protein. The ESM-2-650M and ESM-2-3B models were both trained for PepMLM. Both versions were trained on an NVIDIA 8xA100 640 GB DGX GPU system with Pytorch 2.01 and Python 3.10.10. Specific parameters are shown in Supplementary Table 1.

PepMLM Generation

During the generation phase, the target protein sequence, along with a designated number of mask tokens (at end), was input into the model. Subsequently, the model greedily decodes logits at each masked position to identify peptide binders. To infuse greater diversity into the generation process, top-k sampling was implemented, wherein the model randomly selects the top k highest probability logits at each masked position.

Pseudo-Perplexity of PepMLM

The pseudo-perplexity of ESM-2 was adapted to focus specifically on the evaluation of peptide binder generation. Notably, the perplexity calculation is confined to the binder region, or, in other words, the masked regions. Mathematically, the pseudo-perplexity is defined as:

$$\text{PseudoPerplexity}(b) = \exp \left\{ -\frac{1}{m} \sum_{i=1}^m \log p(b_i | b_{j \neq i}, p) \right\}$$

In this equation, b represents the binder sequence and m is the length of the binder sequence. This modification ensures a more focused evaluation of the generated peptide binders, aligning with the conditional modeling approach adopted in this study.

Generated Peptide Benchmarking

To assess the efficacy of the generated peptide binders, two benchmarking studies were conducted: one on the test set and another on selected critical proteins. In the test set benchmarking, top- k sampling ($k = 3$) was employed to generate a single peptide binder for each target protein. Additionally, the original ESM-2 model was utilized to generate peptides, and random peptides of equivalent length were created. For ESM-2 generation, specifically, mask tokens of the same length were added at the end of target protein sequences for analogous model prediction and decoding as for PepMLM. The perplexity of the PepMLM was compared across four groups. PepMLM-generated binders and test binders were folded using the AlphaFold2 ColabFold version 1.5.2, in conjunction with the protein sequences. Folding metrics including pLDDT and ipTM were gathered, which were utilized to correlate perplexity findings. For each test target protein, the ipTM scores of the test and generated binders were compared to determine the overall hit rate. Notice, as top- k sampling generates with randomness, the hit rate might vary or increase with different runs or k options. For the proteins identified as critical, the model produced eight binders, each of a length of 15 residues, using top- k sampling ($k = 3$). These binders were synthesized for specific target proteins to facilitate subsequent experimental evaluations.

RFDiffusion Generation

In parallel to the PepMLM approach, RFDiffusion was employed to design peptide binders for both cases. For the given test set, RFDiffusion was tasked with generating one peptide binder per target protein, matching the length specified by the ground truth binders. The predicted structures were then converted into sequences using ProteinMPNN with initial guess and number of cycles of 3. For the selected critical proteins, RFDiffusion and ProteinMPNN generated 8 candidate binders, each comprising 15 residues, under identical parameter settings as testset generation. RFDiffusion inference code on ColabFold can be found here: <https://colab.research.google.com/github/sokrypton/ColabDesign/blob/v1.1.1/rf/examples/diffusion.ipynb>

Generation of plasmids

All uAb plasmids were generated from the standard pcDNA3 vector, harboring a cytomegalovirus (CMV) promoter and a C-terminal IRES-mCherry cassette as a transfection control. An Esp3I restriction site was introduced immediately upstream of the CHIPΔTPR CDS and flexible GSGSG linker via the KLD Enzyme Mix (NEB) following PCR amplification with mutagenic primers (Genewiz). For uAb assembly, peptide sequences were human codon-optimized for complementary oligo generation (Genewiz). Oligos were annealed and ligated via T4 DNA Ligase into the Esp3I-digested uAb backbone. Assembled constructs were transformed into 50 μ L NEB Turbo Competent *Escherichia coli* cells, and plated onto LB agar supplemented with the appropriate antibiotic for subsequent sequence verification of colonies and plasmid purification (Genewiz).

Cell culture

A673 cells were maintained in Dulbecco's Modified Eagle's Medium (DMEM) supplemented with 100 units/ml penicillin, 100 mg/ml streptomycin, and 10% fetal bovine serum (FBS). For uAb testing, pcDNA3-uAb (500 ng) plasmids were transfected into cells as triplicates (4×10^5 /well in a 12-well plate) with Lipofectamine 2000 (Invitrogen) in Opti-MEM (Gibco).

Cell fractionation and immunoblotting

On the day of harvest, cells were detached by addition of 0.05% trypsin-EDTA and cell pellets were washed twice with ice-cold 1X PBS. Cells were then lysed and subcellular fractions were isolated from lysates using a 1:100 dilution of protease inhibitor cocktail (Millipore Sigma) in Pierce RIPA buffer (ThermoFisher). Specifically, the protease inhibitor cocktail-RIPA buffer solution was added to the cell pellet, the mixture was placed at 4 °C for 30 min followed by centrifugation at 15,000 rpm for 10 min at 4 °C. The supernatant was collected immediately to a pre-chilled PCR tube, and after adding 4X Bolt™ LDS Sample Buffer (ThermoFisher) with 5% β -mercaptoethanol in a 3:1 ratio, the mixture was incubated at 95 °C for 10 min prior to immunoblotting. Immunoblotting was performed according to standard protocols. Briefly, samples were loaded at equal volumes into Bolt™ Bis-Tris Plus Mini Protein Gels (ThermoFisher) and separated by electrophoresis. iBlot™ 2 Transfer

Stacks (Invitrogen) were used for membrane blot transfer, and following a 1 h room-temperature incubation in SuperBlock™ Blocking Buffer (ThermoFisher), proteins were probed with rabbit anti-4E-BP2 antibody (Cell Signaling, Cat # 2845; diluted 1:500), rabbit anti-Histone 3 antibody (Abcam, Cat # ab1791; diluted 1:500), rabbit anti- β -catenin antibody (Cell Signaling, Cat # 8480; diluted 1:500), mouse anti-TRIM8 antibody (SantaCruz Biotechnology Cat # sc-398878; diluted 1:1000), mouse anti-GAPDH antibody (Santa Cruz Biotechnology, Cat # sc-47724; diluted 1:500), or rabbit anti-Vinculin antibody (ThermoFisher, Cat # 42H89L44; diluted 1:1000) for overnight incubation at 4°C. The blots were washed three times with 1X TBST for 5 min each and then probed with a secondary antibody, goat anti-rabbit IgG (H+L), horseradish peroxidase (HRP) (ThermoFisher, Cat # 31460, diluted 1:5000) or goat anti-mouse IgG (H+L) Poly-HRP (ThermoFisher, Cat # 32230, diluted 1:2000) for 1 h at room temperature. Following three washes with 1X TBST for 5 min each, blots were detected by chemiluminescence using an iBright 1500 Imaging System (ThermoFisher). Densitometry analysis of protein bands in immunoblots was performed using ImageJ software as described here: <https://imagej.nih.gov/ij/docs/examples/dot-blot/>. Briefly, bands in each lane were grouped as a row or a horizontal “lane” and quantified using FIJI’s gel analysis function. Intensity data for the uAb bands was first normalized to band intensity of GAPDH or Vinculin in each lane then to the average band intensity for the uAb vector control cases across replicates.

Statistical analysis and reproducibility

To ensure robust reproducibility of all results, experiments were performed with at least three biological replicates. Sample sizes were not predetermined based on statistical methods but were chosen according to the standards of the field (at least three independent biological replicates for each condition). All data were reported as average values with error bars representing standard deviation (SD). All graphs were generated using Prism 10 for MacOS. No data were excluded from the analyses. The experiments were not randomized. The investigators were not blinded to allocation during experiments and outcome assessment.

Supplementary Figures

Supplementary Figure 1. Top- k sampling.

Supplementary Figure 2. Association between model perplexity and co-folding metrics.

Supplementary Figure 3. Degradation of β -catenin in protein extracts of A673 Ewing sarcoma cells analyzed via immunoblotting.

Supplementary Figure 4. Evaluation of PepMLM-3B.

Supplementary Table 1. Settings and hyperparameters used to train PepMLM-650M.

Supplementary Table 2. Outlier analysis of protein-peptide complexes.

Supplementary Table 3. Peptide sequences and PPL scores for PepMLM experimental testing.

Supplementary Table 4. Peptide sequences and PPL scores for PepMLM vs. RFDiffusion experimental testing.

Author Contributions

T.C. designed the PepMLM architecture, curated peptide-protein data, trained and evaluated trained models. T.C., S.V., V.S.K., R.P., A.H., and P.V. performed *in silico* benchmarking. S.P. conducted *in vitro* assays for uAb screening, with R.W., L.H., T.W., V.Y., E.H. and L.Z. providing technical assistance. P.C. conceived, designed, and directed the study.

Data and Materials Availability

All data needed to evaluate the conclusions in the paper are present in the paper and code repository: <https://github.com/programmablebio/pepmlm>. PepMLM-650M is also hosted on HuggingFace with an easy-to-use demo for peptide generation: <https://huggingface.co/TianlaiChen/PepMLM-650M>.

Competing Interests

P.C. is a co-founder of UbiquiTx, Inc., and is the inventor of patents related to genetically-encoded proteome editing technologies. The remaining authors declare no competing interests.

Acknowledgements

We thank the Duke Compute Cluster and Mark III Systems for providing database resources that have contributed to the research reported within this manuscript. We also thank Manvitha Ponnappati for curating initial peptide datasets.

Declarations

The research was supported by institutional startup funds to the lab of P.C. from Duke University, as well as funds from the Wallace H. Coulter Foundation, the CHDI Foundation, The Hartwell Foundation and NIH grants 3U54CA231630-01A1S4 and 1R21CA278468-01.

References

1. Chen, T., Hong, L., Yudistyra, V., Vincoff, S. & Chatterjee, P. Generative design of therapeutics that bind and modulate protein states. *Curr. Opin. Biomed. Eng.* **28**, 100496 (2023).
2. Zhong, L. *et al.* Small molecules in targeted cancer therapy: advances, challenges, and future perspectives. *Signal Transduction and Targeted Therapy* **6**, 1–48 (2021).
3. Békés, M., Langley, D. R. & Crews, C. M. PROTAC targeted protein degraders: the past is prologue. *Nat. Rev. Drug Discov.* **21**, 181–200 (2022).
4. Dong, G., Ding, Y., He, S. & Sheng, C. Molecular Glues for Targeted Protein Degradation: From Serendipity to Rational Discovery. *J. Med. Chem.* **64**, 10606–10620 (2021).
5. Gao, H., Sun, X. & Rao, Y. PROTAC Technology: Opportunities and Challenges. *ACS Med. Chem. Lett.* **11**, 237–240 (2020).
6. Behan, F. M. *et al.* Prioritization of cancer therapeutic targets using CRISPR-Cas9 screens. *Nature* **568**, 511–516 (2019).
7. Jumper, J. *et al.* Highly accurate protein structure prediction with AlphaFold. *Nature* **596**, 583–589 (2021).
8. Watson, J. L. *et al.* De novo design of protein structure and function with RFdiffusion. *Nature* **620**, 1089–1100 (2023).
9. Gainza, P. *et al.* De novo design of protein interactions with learned surface fingerprints. *Nature* **617**, 176–184 (2023).
10. Vaswani, A. *et al.* Attention is all you need. (2017) doi:10.48550/ARXIV.1706.03762.
11. Ofer, D., Brandes, N. & Linial, M. The language of proteins: NLP, machine learning & protein sequences. *Comput. Struct. Biotechnol. J.* **19**, 1750–1758 (2021).
12. Elnaggar, A. *et al.* ProtTrans: Toward Understanding the Language of Life Through Self-Supervised Learning. *IEEE Trans. Pattern Anal. Mach. Intell.* **44**, 7112–7127 (2022).
13. Madani, A. *et al.* Large language models generate functional protein sequences across diverse families. *Nat. Biotechnol.* **41**, 1099–1106 (2023).
14. Ferruz, N., Schmidt, S. & Höcker, B. ProtGPT2 is a deep unsupervised language model for protein design. *Nat. Commun.* **13**, 1–10 (2022).
15. Rives, A. *et al.* Biological structure and function emerge from scaling unsupervised learning to 250 million protein sequences. *Proc. Natl. Acad. Sci. U. S. A.* **118**, (2021).
16. Lin, Z. *et al.* Evolutionary-scale prediction of atomic-level protein structure with a language model. *Science* **379**, 1123–1130 (2023).
17. Hie, B. L. *et al.* Efficient evolution of human antibodies from general protein language models. *Nat. Biotechnol.* 1–9 (2023).
18. Chatterjee, P. *et al.* Targeted intracellular degradation of SARS-CoV-2 via computationally optimized peptide fusions. *Communications Biology* **3**, 1–8 (2020).
19. Palepu, K. *et al.* Design of Peptide-Based Protein Degradation via Contrastive Deep Learning. *bioRxiv* (2022) doi:10.1101/2022.05.23.493169.

20. Brixi, G. *et al.* SaLT&PepPr is an interface-predicting language model for designing peptide-guided protein degraders. *Communications Biology* **6**, 1–10 (2023).
21. Bhat, S. *et al.* De Novo Generation and Prioritization of Target-Binding Peptide Motifs from Sequence Alone. *bioRxiv* 2023.06.26.546591 (2023) doi:10.1101/2023.06.26.546591.
22. Abdin, O., Nim, S., Wen, H. & Kim, P. M. PepNN: a deep attention model for the identification of peptide binding sites. *Communications Biology* **5**, 1–10 (2022).
23. Martins, P. *et al.* Propedia v2.3: A novel representation approach for the peptide-protein interaction database using graph-based structural signatures. *Front Bioinform* **3**, 1103103 (2023).
24. Steinegger, M. & Söding, J. MMseqs2 enables sensitive protein sequence searching for the analysis of massive data sets. *Nat. Biotechnol.* **35**, 1026–1028 (2017).
25. Mirdita, M. *et al.* ColabFold: making protein folding accessible to all. *Nat. Methods* **19**, 679–682 (2022).
26. Evans, R. *et al.* Protein complex prediction with AlphaFold-Multimer. *bioRxiv* (2021) doi:10.1101/2021.10.04.463034.
27. Johansson-Åkhe, I. & Wallner, B. Improving peptide-protein docking with AlphaFold-Multimer using forced sampling. *Front Bioinform* **2**, 959160 (2022).
28. Zöllner, S. K. *et al.* Ewing Sarcoma-Diagnosis, Treatment, Clinical Challenges and Future Perspectives. *J. Clin. Med. Res.* **10**, (2021).
29. Ding, M. *et al.* The mTOR Targets 4E-BP1/2 Restrain Tumor Growth and Promote Hypoxia Tolerance in PTEN-driven Prostate Cancer. *Mol. Cancer Res.* **16**, 682–695 (2018).
30. Shang, S., Hua, F. & Hu, Z.-W. The regulation of β -catenin activity and function in cancer: therapeutic opportunities. *Oncotarget* **8**, 33972–33989 (2017).
31. Zhao, Z. & Shilatifard, A. Epigenetic modifications of histones in cancer. *Genome Biol.* **20**, 245 (2019).
32. Seong, B. K. A. *et al.* TRIM8 modulates the EWS/FLI oncoprotein to promote survival in Ewing sarcoma. *Cancer Cell* **39**, 1262–1278.e7 (2021).
33. Wang, J. Y. & Doudna, J. A. CRISPR technology: A decade of genome editing is only the beginning. *Science* **379**, eadd8643 (2023).
34. Walton, R. T., Christie, K. A., Whittaker, M. N. & Kleinstiver, B. P. Unconstrained genome targeting with near-PAMless engineered CRISPR-Cas9 variants. *Science* **368**, 290–296 (2020).
35. Zhao, L. *et al.* PAM-flexible genome editing with an engineered chimeric Cas9. *Nat. Commun.* **14**, 1–8 (2023).
36. Vinogradov, A. A., Yin, Y. & Suga, H. Macrocyclic Peptides as Drug Candidates: Recent Progress and Remaining Challenges. *J. Am. Chem. Soc.* **141**, 4167–4181 (2019).
37. Moiola, M., Memeo, M. G. & Quadrelli, P. Stapled Peptides-A Useful Improvement for Peptide-Based Drugs. *Molecules* **24**, (2019).

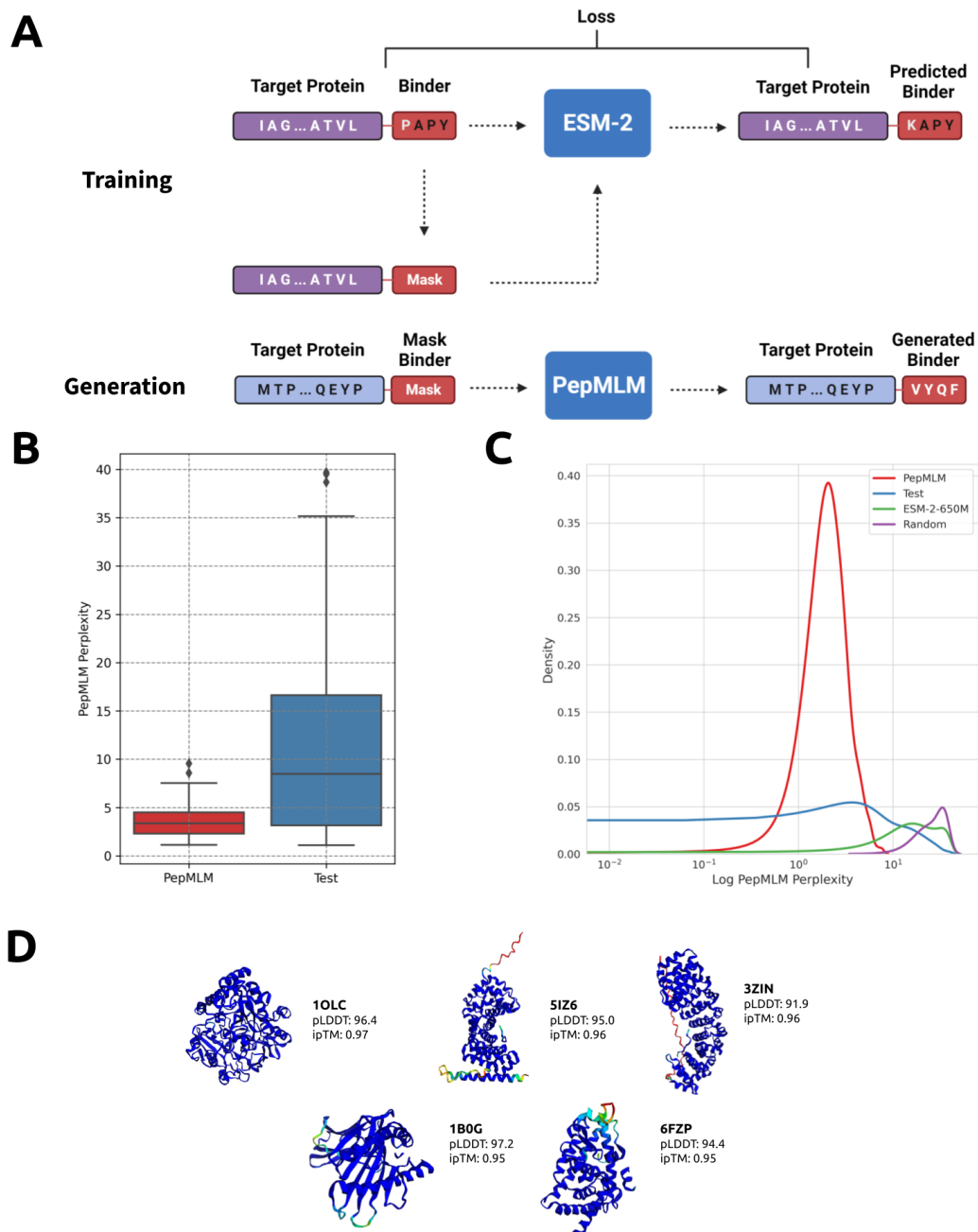


Figure 1. Overview and evaluation of the PepMLM model. (A) The architecture of the PepMLM model. Based on the fine-tuning of ESM-2, the model incorporates the target protein sequence along with a masked binder region during the training phase. During the generation phase, the model can accept target protein sequences and mask tokens to facilitate the creation of peptides of specified lengths. (B) Perplexity distribution comparison. The perplexity values were calculated for test and generated peptides, encompassing the target proteins in the test set. (C) The density distribution visualization of the log perplexity values for target-peptide pairs, encompassing test peptides, PepMLM-650M-generated peptides, ESM-2-650M-generated peptides, and random peptides. (D) AlphaFold-Multimer co-folding examples of specified target proteins from the PDB and sampled peptide binders generated via PepMLM-650M, with the pLDDT values serving as the determinant for color coding. ipTM scores indicate binding stability.

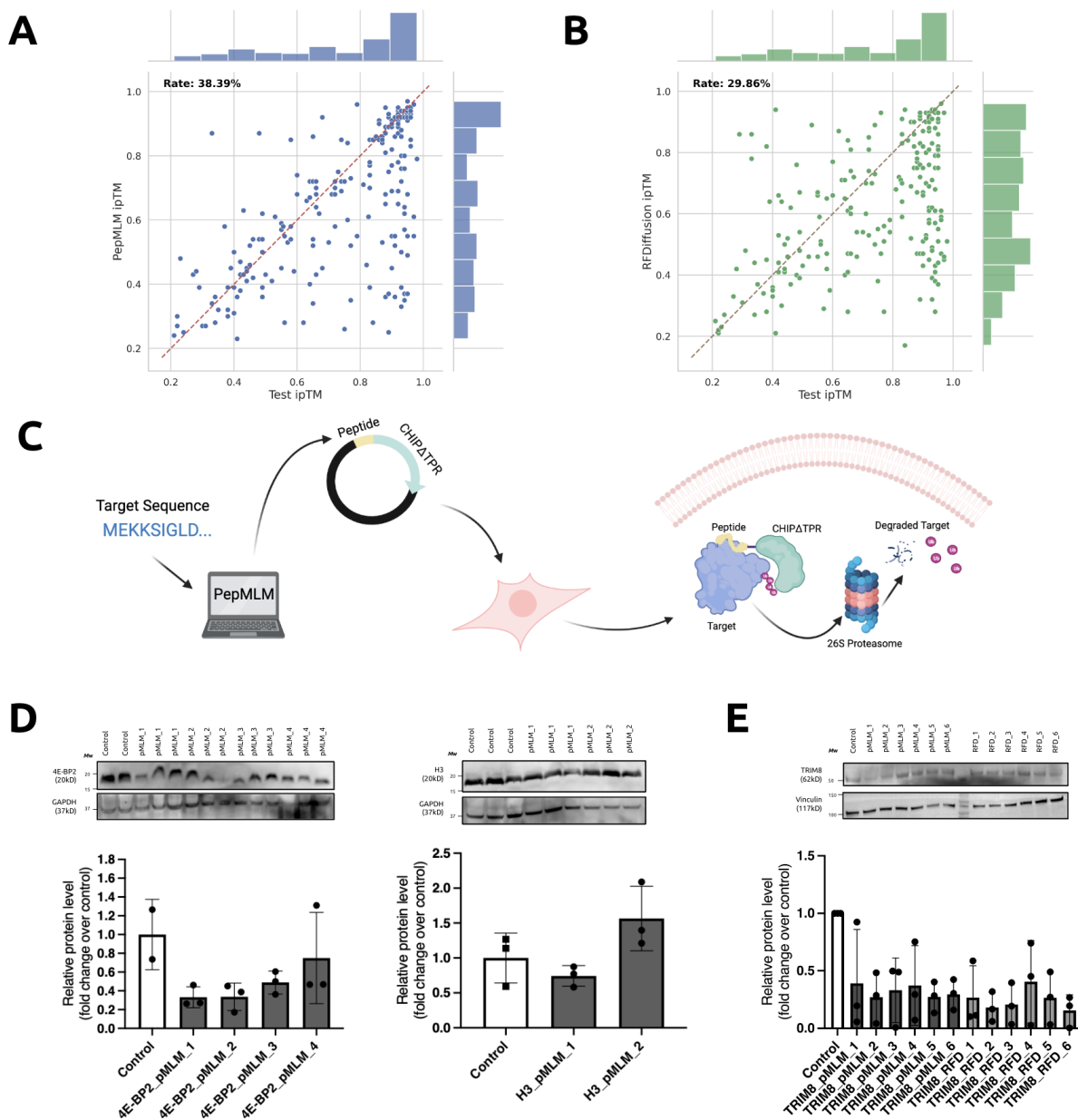


Figure 2. Benchmarking of PepMLM-generated peptides. (A) *In silico* hit-rate assessment of PepMLM. Utilizing AlphaFold-Multimer, ipTM scores were computed for both the generated and test peptides in conjunction with the target protein sequence. The entries are organized in accordance with the ipTM scores attributed to the test set peptides. The hit rate is characterized by the generated peptides exhibiting ipTM scores \geq those of the test peptides. (B) *In silico* hit-rate assessment of RFDiffusion. The analogous assessment was applied for binders generated by RFDiffusion as for PepMLM-derived binders in Part A. (C) Architecture and mechanism of uAb degradation system. CHIP Δ TPR is fused to the C-terminus of PepMLM-designed target-specific peptides, and can thus tag endogenous target proteins for ubiquitin-mediated degradation in the proteasome, post-plasmid transfection. (D) Degradation of endogenous targets in protein extracts of A673 Ewing sarcoma cells analyzed via immunoblotting. Blots are representative of independent transfection replicates ($n = 3$). Relative degradation activity was determined by densitometry analysis of target protein signal normalized to sample-specific GAPDH signal. (E) Degradation of TRIM8 analyzed via immunoblotting. Blots are representative of a single replicate of independent transfection replicates ($n = 3$). Relative degradation activity was determined by densitometry analysis of target protein signal normalized to sample-specific Vinculin signal.

Supplementary Information

PepMLM: Target Sequence-Conditioned Generation of Peptide Binders via Masked Language Modeling

Tianlai Chen,^{1,*} Sarah Pertsemlidis,^{1,*} Rio Watson,¹ Venkata Srikar Kavirayuni,¹ Ashley Hsu,¹ Pranay Vure,¹ Rishab Pulugurta,¹ Sophia Vincoff,¹ Lauren Hong,¹ Tian Wang,¹ Vivian Yudistyra,¹ Elena Haarer,¹ Lin Zhao,¹ Pranam Chatterjee^{1,2,3,†}

1. Department of Biomedical Engineering, Duke University
2. Department of Computer Science, Duke University
3. Department of Biostatistics and Bioinformatics, Duke University

*These authors contributed equally

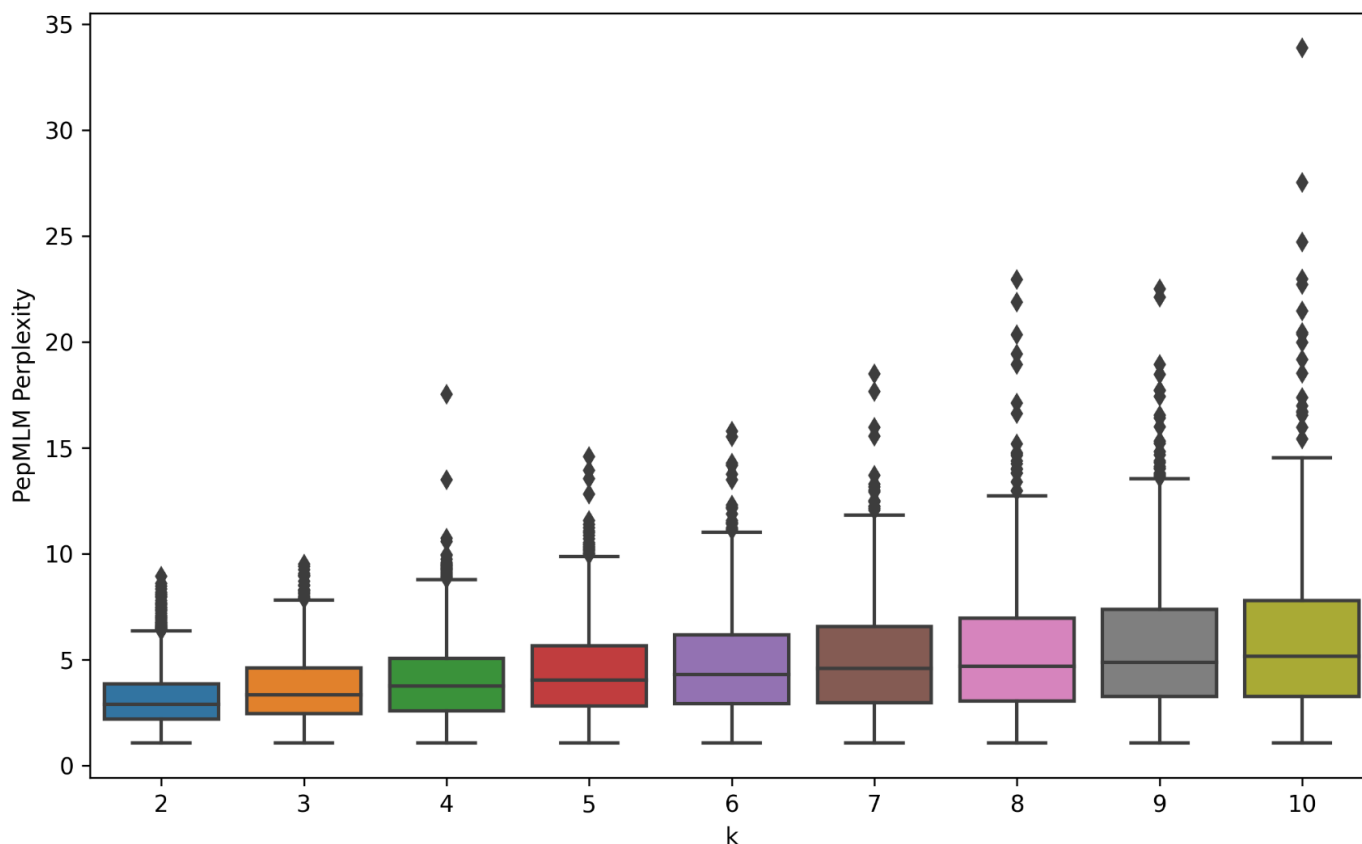
†Corresponding author: pranam.chatterjee@duke.edu

Supplementary Figures

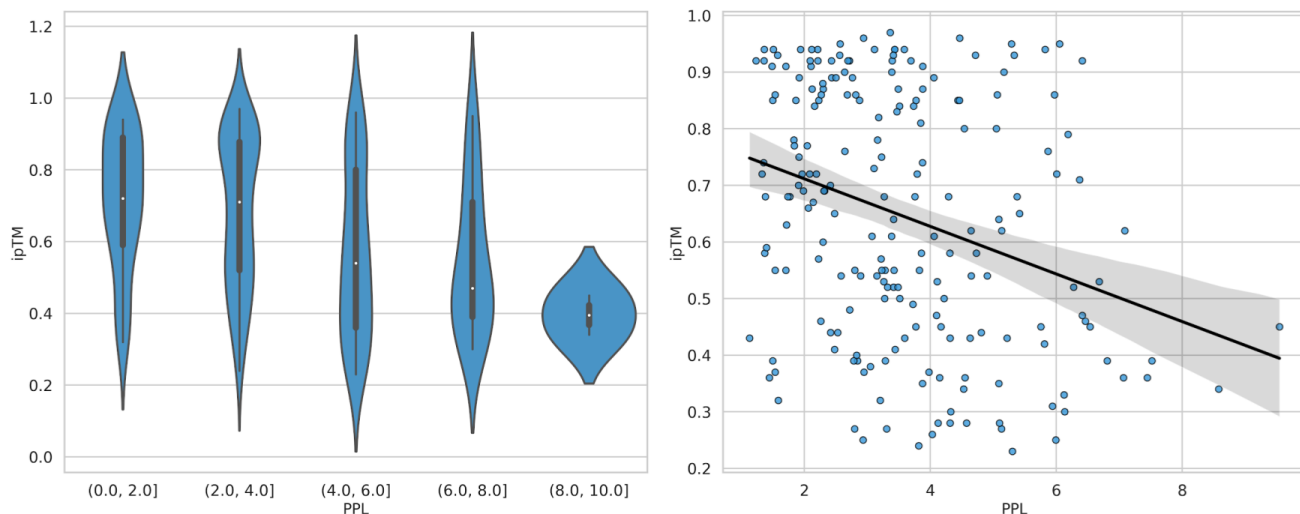
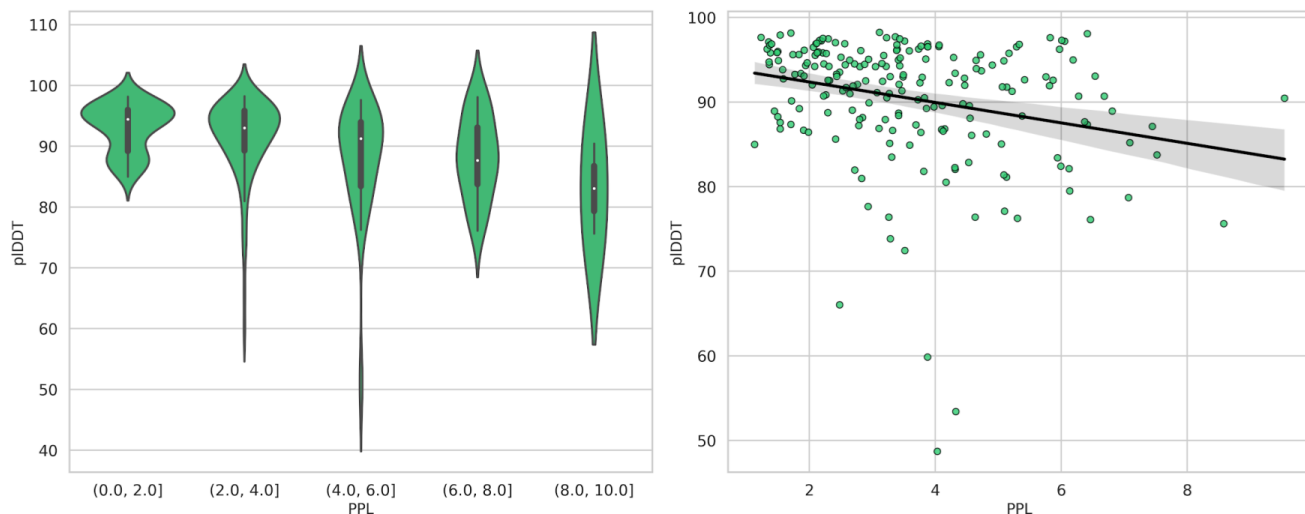
1. Top- k sampling.
2. Association between model perplexity and co-folding metrics.
3. Evaluation of PepMLM-3B.
4. Degradation of β -catenin in protein extracts of A673 Ewing sarcoma cells analyzed via immunoblotting.

Supplementary Tables

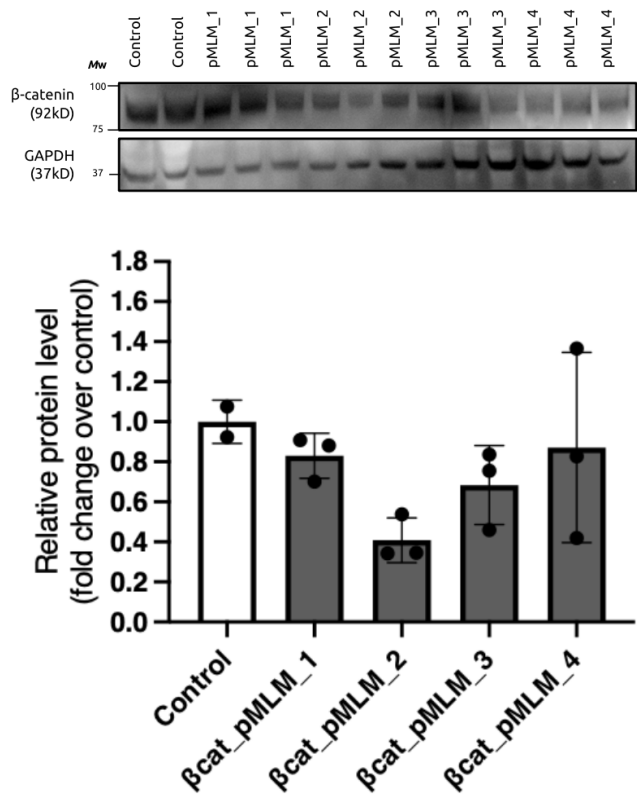
1. Settings and hyperparameters used to train PepMLM-650M.
2. Outlier analysis of protein-peptide complexes.
3. Peptide sequences and PPL scores for PepMLM experimental testing.
4. Peptide sequences and PPL scores for PepMLM vs. RFDiffusion experimental testing.



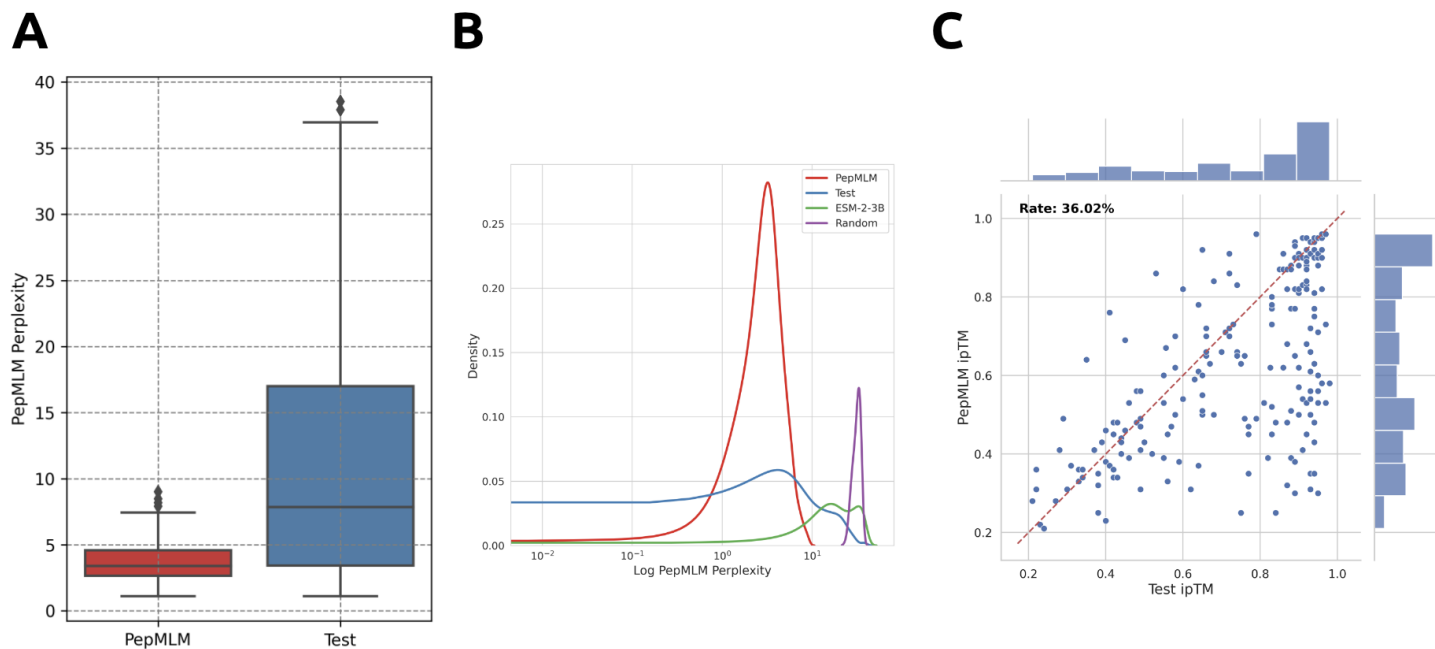
Supplementary Figure 1. Top- k sampling. The chosen k values are plotted against the perplexities determined for target proteins in the test set, based on the generation of 10 binders with lengths matching the reference binder. It was discerned that an escalation in k led to a concomitant rise in perplexity, signifying a diminishment in model assurance. Although elevated k values resulted in augmented diversity of binder sequences, they also manifested a surge in outlier occurrences. To strike an optimal equilibrium between binder sequence diversity and sustained model confidence (evidenced by diminished perplexity), a k value of 3 was adjudged as the preferred choice.

A**B**

Supplementary Figure 2. Association between model perplexity and co-folding metrics. (A) Relationship between ipTM and perplexity (PPL). The initial segment of Figure A presents a violin plot, categorizing perplexity in 2-unit intervals. The subsequent segment delineates the raw data points, accompanied by a regression analysis, indicating a negative correlation (Pearson correlation coefficient -0.30 , $p < 0.001$). The shaded area represents a 95% confidence interval. (B) Negative correlation between PPL and pLDDT, identified by Pearson correlation coefficient of -0.26 ($p < 0.001$). The violin plot underscores a marked decrement in specific folding metrics, most pronounced in ipTM, commensurate with elevated perplexity levels.



Supplementary Figure 3. Degradation of β -catenin in protein extracts of A673 Ewing sarcoma cells analyzed via immunoblotting. Blots are representative of independent transfection replicates ($n = 3$). Relative degradation activity was determined by densitometry analysis of target protein signal normalized to sample-specific GAPDH signal.



Supplementary Figure 4. Evaluation of PepMLM-3B. (A) Perplexity distribution comparison. The perplexity values were calculated for test and generated peptides, encompassing the target proteins in the test set. (B) The density distribution visualization of the log perplexity values for target-peptide pairs, encompassing test peptides, PepMLM-3B-generated peptides, ESM-2-3B-generated peptides, and random peptides. (C) *In silico* hit-rate assessment. Utilizing AlphaFold-Multimer, the ipTM scores were computed for both the generated and test peptides in conjunction with the target protein sequence. The entries are organized in accordance with the ipTM scores attributed to the test set peptides. The hit rate is characterized by the generated peptides exhibiting ipTM scores \geq those of the test set peptides.

Supplementary Table 1. Settings and hyperparameters used to train PepMLM-650M.

Name	Setting
Learning Rate	0.000798
Batch Size	16
Gradient Accumulation	2
Warm up steps	501
Number of training epochs	5
Optimizer	AdamW (default)
Trainer	Default HuggingFace Settings

Supplementary Table 2. Outlier analysis of protein-peptide complexes. This table displays 11 protein-peptide complexes with pseudo-perplexity (PPL) values exceeding 40. Included are evaluation metrics for both the test complexes and the PepMLM generation results, as well as the binder sequences. ipTM scores for test and generated complexes are highlighted in different colors for comparison. Notably, even though these outliers exhibit high PPL values indicative of accurate modeling by PepMLM, the model remains proficient in generating binders that perform equivalently well *in silico* as per AlphaFold-Multimer ipTM score.

PDB ID	Test				PepMLM Generation			
	Binder	PPL	ipTM	pLDDT	Binder	PPL	ipTM	pLDDT
5B5V	FLFGSRSS	47.9	0.45	88.9	YHYVMRYA	3.4	0.52	88.7
4G1C	AVXCAX	72.7	0.86	96.9	TAKXST	2.1	0.91	96.9
2L1C	RAKWDTANNPLXKE ATSTFTNITXRGT	58.1	0.49	61.9	HIAEPPHFFESMQN NYEKPTTYKFQQK	3.2	0.39	73.8
6GHJ	FAQ	160.1	0.71	93.4	MXL	1.8	0.68	93.3
6AMU	MMWDRGLGMM	43.9	0.34	87.9	YQALIGGFNA	4.6	0.28	86.1
5WMR	QIKVRVDMV	64.7	0.91	92.3	LRFWRARTL	5.1	0.86	91.8
5NJC	VLEDRI	98.4	0.83	97.5	AAAAAA	1.4	0.74	97.3
6DQU	GIINTL	126.2	0.87	97.7	YLGANG	2.2	0.84	97.3
2IWB	GHMS	188.7	0.64	96.1	XPPX	2.1	0.67	95.9
4C78	GVMRRL	42.8	0.94	92.1	SSGVMR	2.2	0.57	90.7
3M5M	FDEMEEC	101.9	0.93	97.2	SECVTCC	2.1	0.94	96.9

Supplementary Table 3. Peptide sequences and PPL scores for PepMLM experimental testing.

Target	UniProt ID	uAb Name	Peptide Sequence	PPL
4E-BP2	Q13542	4E-BP2_pMLM_1	DSTIVVQTK	5.365092
4E-BP2	Q13542	4E-BP2_pMLM_2	DSSIVVQTP	6.203168
4E-BP2	Q13542	4E-BP2_pMLM_3	ESTIVVTTP	6.035627
4E-BP2	Q13542	4E-BP2_pMLM_4	DDTLVVTTP	6.283843
Histone 3	P68431	H3_pMLM_1	DEDY	2.653573
Histone 3	P68431	H3_pMLM_2	DEEY	3.240149
β -catenin	P35222	β cat_pMLM_1	KKALQL	4.541961
β -catenin	P35222	β cat_pMLM_2	GKTFQV	5.699396
β -catenin	P35222	β cat_pMLM_3	GKALQV	4.793907
β -catenin	P35222	β cat_pMLM_4	KATLKL	5.595168

Supplementary Table 4. Peptide sequences and PPL scores for PepMLM vs. RFDiffusion experimental testing.

Target	UniProt ID	uAb Name	Peptide Sequence	PPL
TRIM8	Q9BZR9	TRIM8_pMLM_1	TSTAPGLYSKEVTSS	6.878241
TRIM8	Q9BZR9	TRIM8_pMLM_2	QQPPLGLSLSLVSP	5.892988
TRIM8	Q9BZR9	TRIM8_pMLM_3	TSPPEDLYRKEGTPL	5.646809
TRIM8	Q9BZR9	TRIM8_pMLM_4	MSRALDLLRSATTLP	5.739593
TRIM8	Q9BZR9	TRIM8_pMLM_5	MRPGEKLLRSETTPS	4.332752
TRIM8	Q9BZR9	TRIM8_pMLM_6	MRPAEGLLRKLVSPS	4.600287
TRIM8	Q9BZR9	TRIM8_RFD_1	SLRELEEEFLAELKK	24.99706268
TRIM8	Q9BZR9	TRIM8_RFD_2	KELEEKVEEIKKLLA	30.01940536
TRIM8	Q9BZR9	TRIM8_RFD_3	SEIEEQIEELKKLLE	42.00793076
TRIM8	Q9BZR9	TRIM8_RFD_4	MEKYKELIEAAKELE	45.64295197
TRIM8	Q9BZR9	TRIM8_RFD_5	KEIEEQIEELKKLEA	45.76978302
TRIM8	Q9BZR9	TRIM8_RFD_6	SLEAIKKVIEEAREL	47.95458603